

Laser-assisted Analytical Chemistry and Mass Spectrometry

Renato Zenobi*

Abstract: This article summarizes the current research of our group. Our activities are focused in three main areas, (i) the application of soft ionization mass spectrometry to a range of analytical problems, (ii) the development and fundamental understanding of laser mass spectrometric methods and processes, and (iii) the development of near-field optical microscopy and spectroscopy for nanodiagnostic and nanoanalytical purposes. References to the original literature from our group are given. Extended and continuously updated information can be found in these references as well as on our group web page under <http://www.ceac.ethz.ch/zenobi/>.

Keywords: Electrospray ionization · MALDI · Mass spectrometry · Scanning near-field optical microscopy

Novel Applications of Laser-assisted Mass Spectrometry

The term ‘laser mass spectrometry’ has for many become virtually synonymous with molecular weight determination and sequencing of biopolymers, mostly proteins, by matrix-assisted laser desorption/ionization time-of-flight (MALDI-TOF) mass spectrometry. Indeed, MALDI is one of the celebrated soft ionization methods in modern mass spectrometry. It is very widely used, but its range of applications goes far beyond biopolymer analysis. Furthermore, both in our laboratory and elsewhere, a range of alternative laser mass spectrometric methodologies are being applied in areas where MALDI would be unsuitable. Our group has never been involved in the technology of biopolymer sizing and sequencing by MALDI-MS. Rather, the ‘niche’ in our laboratory for the application of soft ionization mass spectrometry to problems in biology and biochemistry is the study of **noncovalent interactions**. By using soft ionization conditions and proper sample preparation protocols, noncovalently

bound aggregates and complexes are found to survive the vaporization and ionization steps and have thus become accessible for MS analysis.

Both MALDI and electrospray ionization (ESI) can be used for studying molecular recognition and supramolecular chemistry, for investigating interactions that form the basis of the function of biomacromolecules, for screening of potential therapeutic agents, and as a diag-

nostic in the emerging area of molecular machines and molecular computers. In contrast to more conventional solution phase analytical methods, mass spectrometry is fast and very sensitive. It will therefore be of particular value for addressing problems in a situation when the amount of sample is limited.

Fig. 1 shows an overlay of two electrospray ionization mass spectra of myoglobin, recorded under denaturing (left

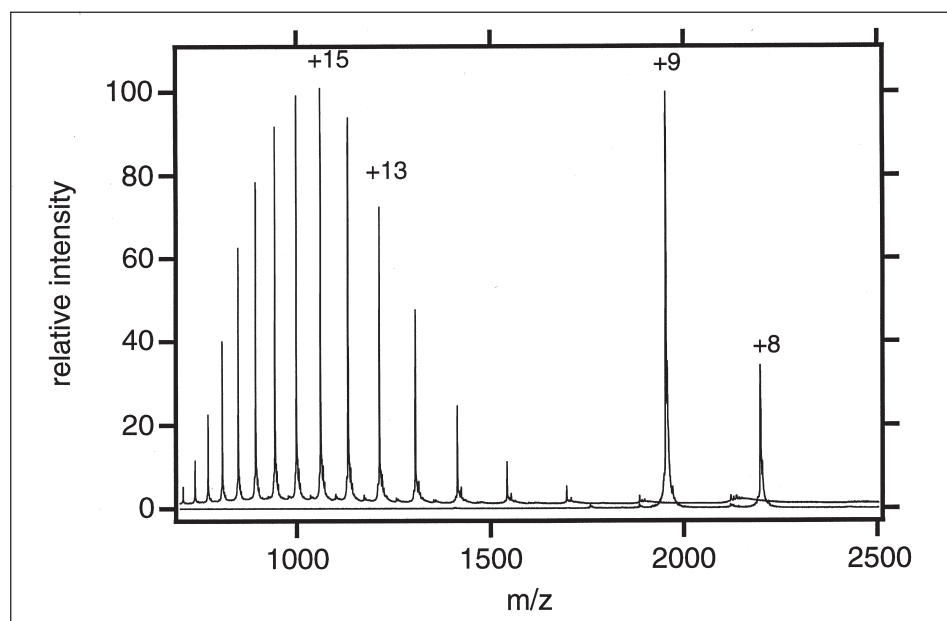


Fig. 1. Positive ion mode nanospray ESI mass spectrum of denatured myoglobin (left hand, high charge state distribution; $M = 16957 \pm 1$ Da) and of native myoglobin (right hand, low charge state distribution; $M = 17570 \pm 2.5$ Da). The mass difference of 614.5 Da corresponds to the noncovalently bound heme cofactor.

*Correspondence: Prof. Dr. R. Zenobi
Department of Chemistry
Swiss Federal Institute of Technology
ETH Hönggerberg
CH-8093 Zürich
Tel.: +41 1 632 43 76
Fax: +41 1 632 12 92
E-Mail: zenobi@org.chem.ethz.ch

side) and 'native' (right side) solution conditions. The most striking difference is the much higher charge state for the denatured myoglobin, reflecting the larger number of exposed basic amino acid residues available for protonation. Another difference is the deconvoluted mass, which decreases by 614.5 Da when going from native to denaturing conditions. This mass difference corresponds exactly to the loss of noncovalently bound heme, the cofactor that is apparently lost upon denaturation.

We are investigating other, more complex enzyme-ligand systems, and we are developing methods for specific recognition of exposed acidic and basic amino acid residues on the surface of proteins by complexing them with suitable ligands [1]. Specially tailored chemical controls are used in these studies to ensure that a *specific* noncovalent complex – rather than a nonspecific gas phase adduct or cluster – is probed in the mass spectrometric experiment. A recurring question concerns the strength of noncovalent interactions. We are in the process of developing MS methods to measure noncovalent binding energies.

In a different project, we are applying a special MALDI sample preparation method, two-phase MALDI, to the chemical analysis of triterpenoids that occur in varnishes on old master paintings [2][3]. This research is carried out in collaboration with the Schweizerisches Institut für Kunstwissenschaft (Zürich), the Berner Fachhochschule, and the Kunsthau Zürich. In regular MALDI, a sample is co-crystallized with an excess of a solid organic matrix. In two-phase MALDI, the matrix consists of a mixture of fine (1–2 µm diam.) particulates and the sample plus, sometimes, some cationization agent and a vacuum-stable liquid as a binder and medium for desorption/ionization. This method turned out to be rather generally applicable, even for fairly nonpolar compounds. It is very well suited to study the triterpenoid compounds that form the main constituents of varnishes on paintings. The aging of these varnishes results in yellowing and cracking, which means that they have to be removed and replaced in regular intervals of about 50 years. Chemically speaking, oxidation and polymerization, followed by chemical degradation are the processes that are observed by our analytical method. Our goal is to come up with practical guidelines for restorers to eliminate the need for replacing the varnish, or at least to greatly extend its lifetime, by making recommendations about the stor-

age conditions for the paintings and about the raw materials for varnishes.

Finally, we have developed a method named **Two-Step Laser Mass Spectrometry (L2MS)** which combines infrared laser induced desorption of neutral analyte molecules followed by resonance-enhanced multiphoton ionization by a second, ultraviolet laser pulse. This ionization process is highly efficient, optically selective and soft, resulting in mass spectra dominated by parent ion peaks of classes of compounds selected by the choice of the ionization laser wavelength. For example, using a wavelength range of 250 ... 270 nm, polycyclic aromatic hydrocarbons (PAHs) and related species with aromatic chromophores are easily and efficiently ionized, whereas other substances such as aliphatic compounds are strongly discriminated against. L2MS is therefore an interesting method for the direct chemical analysis of complex mixtures.

In our laboratory, L2MS is mostly applied to environmental chemistry and problems related to pollution. For example, we used L2MS to quantify contaminants in natural water samples. The only sample preparation method consisted in freezing about 200 µl of water in a small sample dish that was directly inserted into the L2MS ion source [4]. Detection limits ($S/N = 3$) were in the low-microgram per liter range for most compounds investigated, *e.g.* phenol, naphthalene, fluorene, phenanthrene, methylphenanthrene, pyrene, 9,10-dimethylanthracene, 1-methylpyrene, benzo(a)anthracene, and

benzo(a)pyrene. L2MS was also used for the direct chemical analysis of adsorbates on aerosol particles. In this project the samples were collected by pumping air through a quartz fiber filter mounted in a holder that could be directly transferred to the L2MS ion source. Aerosols from both well-defined emission sources (diesel engines, gasoline engines, residential heating, wood fires, and cigarettes) and from two urban field sites were investigated [5][6]. In the field study, we were able to limit sample collection time to only 15 min, allowing the dynamic behavior of PAHs and other polycyclic aromatic compounds to be followed quantitatively over the course of different days. Using specific marker peaks in the L2MS data, diesel and gasoline emissions could be clearly identified as major contributors to urban aerosols collected next to a street with heavy traffic (30 000 vehicles/day), but they were also evident in an urban background site in a nearby city park.

The following example originates from another study, in which aerosols formed from cigarette smoke were collected and analyzed. We studied mainstream smoke (inhaled and exhaled by a smoker), sidestream smoke (from the burning cigarette), and air in the smoking lobby of our former institute building. It was found that ion signals at m/z 118, 132, 146, 160, and 174 were unique to environmental tobacco smoke in their presence and intensity (see Fig. 2). They are interpreted as indazole, benzimidazole, or indane ($m/z = 118$) and their alkylated substituents ($m/z = 132, 146,$

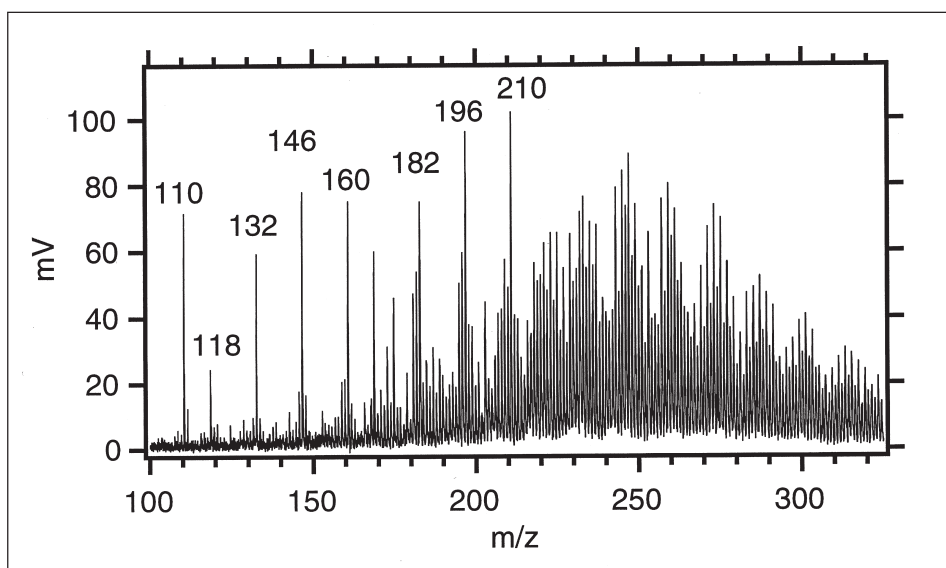


Fig. 2. Average mass spectra from filter samples collected from the smoking lobby between 9:30 and 10:00 CET. This period represents the peak morning ion signal for the environmental tobacco smoke tracer ions (between $m/z = 110$ and 196) as well as the peak in the number of smokers present.

160, 174). $m/z = 146$ can also be assigned to myosmine. All these compounds are known to occur in tobacco smoke. For the smoking lobby these ions were found to be present as soon as the first smokers appeared and persisted over the course of the day. Aerosol samples taken in the morning prior to the presence of smokers in the lobby reveal the presence of skeletal PAHs, indicative of outdoor urban traffic aerosol penetration into the building.

A somewhat puzzling recent finding was that tobacco marker peaks could be detected in aerosols collected in a very remote area, at the High Alpine Research Station on Jungfraujoch. Two possible sources exist, either long-range transport (in particular, by convection), or local contamination from the observation deck where visitors have access. If the latter is indeed dominant, it would mean that smokers among the tourists visiting the Jungfraujoch each day negatively affect the air quality even in a supposedly pristine site in the Swiss Alps.

Methods Development and Fundamentals of Laser Mass Spectrometry

Our group is continuously improving both **MS instrumentation** as well as **sample preparation methods** for laser-assisted mass spectrometry. We have recently described a method for producing MALDI samples from insoluble analyte molecules such as polymers. It is based on pressing a pellet from a mixture of finely ground analyte and matrix powder [7]. Another example is the liquid/solid two-phase matrices mentioned above [8][9]. A possible future development could be to sinter the particulate phase of these two-phase matrices into the shape of a small frit and to deliver a liquid sample stream to the ion source of a laser desorption mass spectrometer through this frit. This concept would essentially allow direct on-line interfacing of liquid separations with laser desorption mass spectrometry or MALDI. First attempts towards this goal have been made in our group [10], but there is still much room for improvement before such an interface will become easily and generally applicable.

An active area in our laboratory is the investigation of fundamental molecular processes that are responsible for **ion formation in MALDI** [11]. Matrix-assisted laser desorption/ionization has been developed empirically, and despite its

widespread use, the factors that decide the success or failure of MALDI experiments are incompletely understood. We wish to understand MALDI well enough that it can be rationally and systematically developed to have greater sensitivity, wider applicability, higher reliability, and perhaps even be used quantitatively. Our working hypothesis is that both primary and secondary steps in the ion formation control the outcome of a MALDI MS experiment. By primary steps we mean the initial processes leading to charge separation upon the action of the laser pulse on the MALDI sample, for example liberation of pre-formed ions [12], energy pooling [13] or multicenter models, excited state proton transfer, disproportionation, multiphoton ionization, or break-up of the sample into charged chunks and clusters. Secondary steps are in-plume ion-molecule reactions that convert the initially formed charged species to the ions that are observed in the MALDI mass spectrum [14]. We hypothesize that primary ionization steps can be completely masked by secondary, in-plume reactions that may include proton, cation, or electron transfer reactions, or charged particle ejection.

These mechanistic studies depend on the availability of photochemical, photo-physical and thermodynamic data on MALDI matrices, their fragments, and clusters, which has been hard to come by in the past. We have thus embarked in a program to determine the important parameters in our laboratory. Some of this research is the subject of an independent project led by Dr. R. Knochenmuss and involves the use of **molecular beam methods**, to investigate either free matrix molecules or aggregates of matrix and analyte. They can be examined in detail, in the gas phase, without the complications of the desorption event and plume. Applying modern laser spectroscopy and time-resolved methods [15] fundamental properties of these species such as ionization potentials [16] or fluorescence lifetimes can be measured, and the basic physicochemical steps in the MALDI ionization process can be isolated.

Thermodynamic properties of MALDI matrices are also being measured using **Fourier-Transform Ion Cyclotron Resonance (FT-ICR) Mass Spectrometry**. FT-ICR mass spectrometry boasts a mass resolution exceeding $M/\Delta M = 10^6$, suitable for addressing problems that cannot be studied by the lower resolution TOF mass spectrometers that are typically employed for laser-assisted MS. Furthermore, the FT-ICR is a magnetic ion

trap that allows ion-molecule reactions to be investigated. We have been using so-called bracketing methods to determine gas-phase proton affinities [17] [18], basicities, and metal ion affinities of MALDI matrices, matrix anions, matrix fragments, and matrix clusters. As an example, Fig. 3 shows that the gas-phase basicity of sinapic acid anions in monomeric and dimeric form differs by as much as 1 eV. Considering disproportionation reactions in a MALDI plume, for example $M + M \rightarrow [M + H]^+ + [M - H]^-$, the measured values for the gas-phase basicity of M and $[M - H]^-$ allows us to determine the energy requirements for this and similar reactions [19]. For sinapic acid, proton disproportionation between monomeric species costs 5.59 eV, whereas the energy requirement for the reaction involving the dimer, $M_2 + M \rightarrow [M + H]^+ + [M_2 - H]^-$, is endothermic by only 4.4 eV. Finally, proton transfer of the sinapic acid dimer to an analyte molecule may cost as little as 3 eV, less than the energy available from one MALDI laser photon.

Recently, we have become active in the development of new FT-ICR traps, most notably open geometry 'dynamic' traps [20][21]. These have already shown promise for efficient trapping of laser-desorbed (MALDI) ions. The open trap geometry should also permit simultaneous optical experiments such as fluorescence studies on mass-selected ions stored in the FT-ICR cell.

Nanochemical Analysis and Nanodiagnosics Using Near-Field Optical Microscopy and Spectroscopy

Researching the nanometer scale is currently of great relevance in many branches of modern science and engineering. As nanoscience and nanotechnology develop, powerful nanodiagnostic tools capable of recording chemical information with nanometer spatial resolution will become increasingly important [22]. Scanning tunneling microscopy and atomic force microscopy usually do not give any chemical information. By combining scanning near-field optical microscopy (SNOM) – the 'optical member' of the family of scanning probe microscopies – with optical spectroscopy, it is possible to obtain molecular information from sample areas as little as 50 nm in diameter. SNOM is based on a sub-wavelength light source that is scanned above the object of interest at a distance

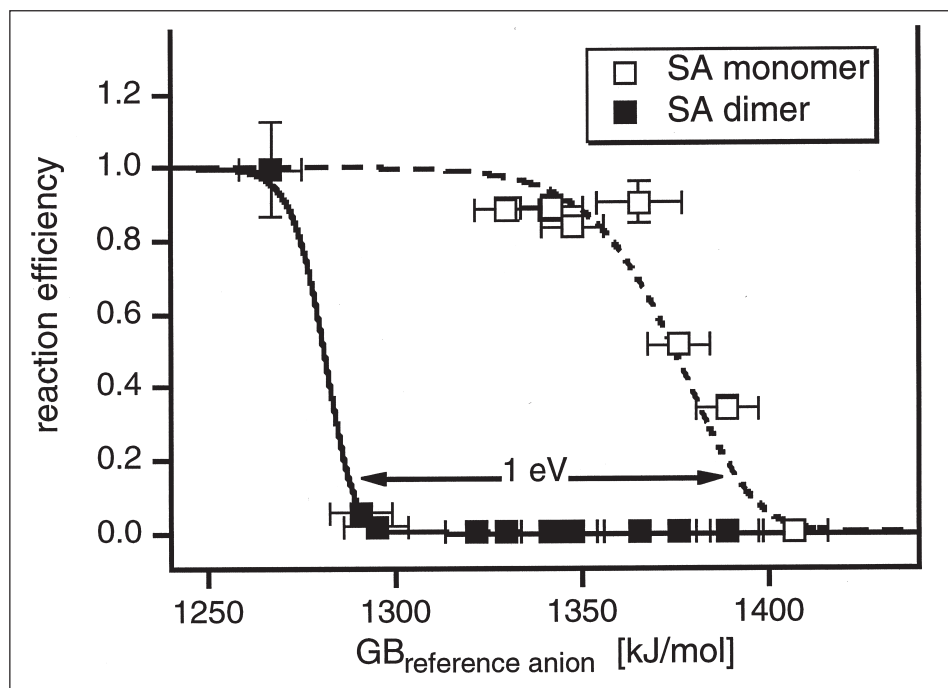


Fig. 3. Bracketing reaction efficiencies as a function of reference anion gas-phase basicity for the sinapic acid anion and the sinapic acid dimer anion. The dashed lines are fits. Adapted from [18].

of a few nm. In the optical near field, the illuminated area is not limited by diffraction, but merely by the size of the illumination source. We are using high quality SNOM probes allowing not only high resolution optical imaging, but also localized spectroscopic investigations of surfaces thanks to their high optical throughput.

The usual form of **SNOM imaging** employs fluorescence. A disadvantage of fluorescence imaging is that a fluorescent moiety or fluorescent label must be present, which is not always possible. A further shortcoming is that fluorescence spectra are broad and unstructured and do not reveal much chemical detail. A viable alternative is vibrational spectroscopy,

i.e. infrared or Raman. An example of such a spectroscopic investigation is shown in Fig. 4. A silver island film (large islands) on a glass substrate was covered with a thin, uniform layer of Rhodamine 6G, and the Raman spectrum was taken at several positions on the sample surface indicated by the dark circles [23]. Excitation was by using the 488 nm

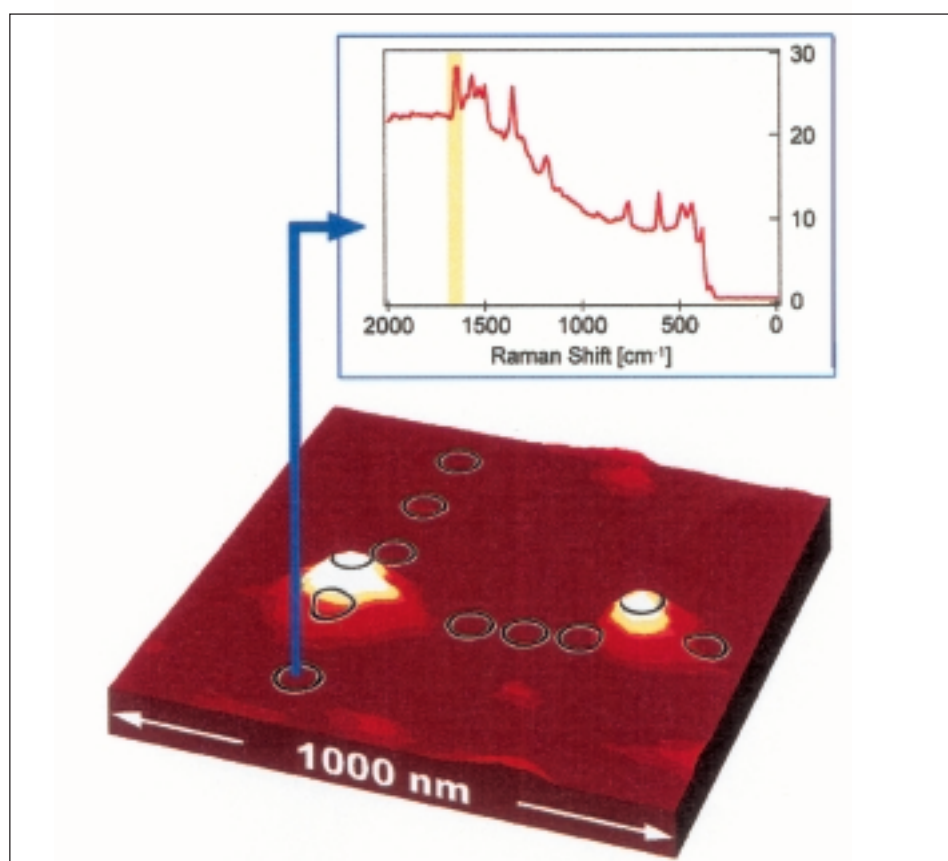


Fig. 4. Topographic image of a SERS silver island substrate used for the near-field Raman measurements. The circles are 70 nm in diameter and represent an estimate of the optical resolution obtained with the SNOM tip used. The inset represents the SERS spectrum obtained at the location indicated by the blue arrow. The vibrational bands detected correspond to those of Rhodamine 6G. Adapted from [23].

line from an Ar⁺ laser directed at the sample by a SNOM fiber tip with an opening of only 70 nm diameter. The Raman scattered light was collected with a microscope objective and analyzed in an optical spectrograph. The silver islands give rise to strong enhancement of the Raman scattering, an effect known as surface enhanced Raman scattering (SERS). Thus, sharp lines originating from the vibrational modes of Rhodamine 6G can be seen with appreciable intensity, superimposed on a broad fluorescence background.

The latest addition to our suite of nano-diagnostic tools is optical 'nanosampling' by pulsed **laser ablation through a near-field optical tip**. The ablated material can be transported over a distance of a few micrometers, collected, and analyzed with a complementary, highly sensitive analytical method such as mass spectrometry. We have recently realized an MS interface for this purpose [24]. It consisted of a 20 μm i.d. stainless steel capillary welded to the tapered end of a 20 cm long, 10 mm i.d. stainless steel tube that was pointing directly towards the electron impact ionizer of a quadrupole mass spectrometer (QMS) ion source. The capillary inlet was positioned very close (< 5 μm) to the SNOM tip using a microactuator, and the sample was tilted towards the capillary for better sampling efficiency. The interface is essentially a controlled leak, which puts some demands on the vacuum pumps. With a 2000 l/s oil diffusion pump, we were able to maintain an operating pressure of better than $5 \cdot 10^{-5}$ mbar in the main chamber, more than sufficient to operate the QMS. The stainless steel tube could be heated to 260 °C to prevent clogging of the orifice and prolonged adsorption of ablation products to its inner wall. The sensitivity of this set-up was found to be sufficiently high for individual near-field ablation events to be detected. The sample chosen for this experiment was a bis-[phenyl-N,N-diethyltriazene]-ether. This compound is designed to decompose into nitrogen and other gaseous products upon absorption of pulsed UV laser light. We thus detected the transient signal of N₂ with the QMS tuned to $m/z = 28$. In the future, a miniature ion trap positioned very close to the interface could be used to accumulate as many ions as possible and to scan the mass spectrum after each ablation pulse. We are also interested in learning whether the liberated material is in the form of intact molecules, and in obtaining mass resolved images of surfaces by scanning

the SNOM ablation probe over the sample.

Acknowledgments

This work would not have been possible without a large number of diligent and dedicated coworkers. In particular, I am indebted to Drs. R. Knochenmuss, V. Deckert, and M. Kalberer for their help with running the laboratory. I thank J. Daniel, B. Morrical, K. Breuker, and R. Stöckle whose results are depicted in the figures shown, and all the past and current members of the group for their contributions. Generous financial support from the Swiss National Science Foundation, the ETH Zurich, and Ciba (now Novartis) is gratefully acknowledged.

Received: June 18, 2001

- [1] S.D. Friess, R. Zenobi, *J. Am. Soc. Mass Spectrom.* **2001**, *12*, 810–818.
- [2] P. Dietemann, M.J. Edelmann, C. Meisterhans, C. Pfeiffer, S. Zumbühl, R. Knochenmuss, R. Zenobi, *Helv. Chim. Acta* **2000**, *83*, 1766–1777.
- [3] P. Dietemann, M. Kälin, S. Zumbühl, R. Knochenmuss, S. Wülfert, R. Zenobi, *Anal. Chem.* **2001**, *73*, 2087–2096.
- [4] T.D. Bucheli, O.P. Haefliger, R. Dietiker Jr., R. Zenobi, *Anal. Chem.* **2000**, *72*, 3671–3677.
- [5] O.P. Haefliger, T.D. Bucheli, R. Zenobi, *Environm. Sci. Technol.* **2000**, *34*, 2178–2183.
- [6] O.P. Haefliger, T.D. Bucheli, R. Zenobi, *Environm. Sci. Technol.* **2000**, *34*, 2184–2189.
- [7] R. Skelton, F. Dubois, R. Zenobi, *Anal. Chem.* **2000**, *72*, 1707–1710.
- [8] M.J. Dale, R. Knochenmuss, R. Zenobi, *Anal. Chem.* **1996**, *68*, 3321–3332.
- [9] M.J. Dale, R. Knochenmuss, R. Zenobi, *Rapid Commun. Mass Spectrom.* **1997**, *11*, 136–142.
- [10] H. Ørsnes, R. Zenobi, *Chem. Soc. Rev.* **2001**, *30*, 104–112.
- [11] R. Zenobi, R. Knochenmuss, *Mass Spectrom. Rev.* **1999**, *17*, 337–366.
- [12] E. Lehmann, R. Knochenmuss, R. Zenobi, *Rapid Commun. Mass Spectrom.* **1997**, *11*, 1483–1492.
- [13] R. Knochenmuss, F. Dubois, M.J. Dale, R. Zenobi, *Rapid Commun. Mass Spectrom.* **1996**, *10*, 871–877.
- [14] R. Knochenmuss, A. Stortelder, K. Breuker, R. Zenobi, *J. Mass Spectrom.* **2000**, *35*, 1237–1245.
- [15] R. Knochenmuss, A. Vertes, *J. Phys. Chem. B* **2000**, *104*, 5406–5410.
- [16] V. Karbach, R. Knochenmuss, *Rapid Commun. Mass Spectrom.* **1998**, *12*, 968–974.
- [17] R.J.J.M. Steenvoorden, K. Breuker, R. Zenobi, *Eur. Mass Spectrom.* **1997**, *3*, 339–346.
- [18] K. Breuker, R. Knochenmuss, R. Zenobi, *Int. J. Mass Spectrom.* **1998**, *184*, 25–38.
- [19] K. Breuker, R. Knochenmuss, R. Zenobi, *J. Am. Soc. Mass Spectrom.* **1999**, *10*, 1111–1123.
- [20] V. Frankevich, R. Zenobi, *Rapid Commun. Mass Spectrom.* **2001**, *15*, 979–985.

- [21] V. Frankevich, R. Zenobi, *Int. J. Mass Spectrom.* **2001**, *207*, 57–67.
- [22] R. Zenobi, V. Deckert, *Angew. Chem. Intl. Ed.* **2000**, *39*, 1746–1756.
- [23] R.M. Stöckle, V. Deckert, C. Fokas, D. Zeisel, R. Zenobi, *Vibr. Spec.* **2000**, *22*, 39–48.
- [24] R. Stöckle, P. Setz, V. Deckert, T. Lippert, A. Wokaun, R. Zenobi, *Anal. Chem.* **2001**, *73*, 1399–1402.